



The Effect of Front-Side Silver Metallization on Underlying $n^+ - p$ Junction in Multicrystalline Silicon Solar Cells

Preprint

C.-S. Jiang, H.R. Moutinho, and M.M. Al-Jassim
National Renewable Energy Laboratory

Z.G. Li, L. Liang, and A. Ionkin
DuPont Central Research and Development

*Presented at the 2012 IEEE Photovoltaic Specialists Conference
Austin, Texas
June 3–8, 2012*

NREL is a national laboratory of the U.S. Department of Energy, Office of Energy Efficiency & Renewable Energy, operated by the Alliance for Sustainable Energy, LLC.

Conference Paper
NREL/CP-5200-54112
June 2012

Contract No. DE-AC36-08GO28308

NOTICE

The submitted manuscript has been offered by an employee of the Alliance for Sustainable Energy, LLC (Alliance), a contractor of the US Government under Contract No. DE-AC36-08GO28308. Accordingly, the US Government and Alliance retain a nonexclusive royalty-free license to publish or reproduce the published form of this contribution, or allow others to do so, for US Government purposes.

This report was prepared as an account of work sponsored by an agency of the United States government. Neither the United States government nor any agency thereof, nor any of their employees, makes any warranty, express or implied, or assumes any legal liability or responsibility for the accuracy, completeness, or usefulness of any information, apparatus, product, or process disclosed, or represents that its use would not infringe privately owned rights. Reference herein to any specific commercial product, process, or service by trade name, trademark, manufacturer, or otherwise does not necessarily constitute or imply its endorsement, recommendation, or favoring by the United States government or any agency thereof. The views and opinions of authors expressed herein do not necessarily state or reflect those of the United States government or any agency thereof.

Available electronically at <http://www.osti.gov/bridge>

Available for a processing fee to U.S. Department of Energy and its contractors, in paper, from:

U.S. Department of Energy
Office of Scientific and Technical Information

P.O. Box 62
Oak Ridge, TN 37831-0062
phone: 865.576.8401
fax: 865.576.5728
email: <mailto:reports@adonis.osti.gov>

Available for sale to the public, in paper, from:

U.S. Department of Commerce
National Technical Information Service
5285 Port Royal Road
Springfield, VA 22161
phone: 800.553.6847
fax: 703.605.6900
email: orders@ntis.fedworld.gov
online ordering: <http://www.ntis.gov/help/ordermethods.aspx>

Cover Photos: (left to right) PIX 16416, PIX 17423, PIX 16560, PIX 17613, PIX 17436, PIX 17721



Printed on paper containing at least 50% wastepaper, including 10% post consumer waste.

The Effect of Front-Side Silver Metallization on Underlying n^+p Junction in Multicrystalline Silicon Solar Cells

C.-S. Jiang,¹ Z.G. Li,² H.R. Moutinho,¹ L. Liang,² A. Ionkin,² and M.M. Al-Jassim¹

¹National Renewable Energy Laboratory, Golden, CO 80401, USA

²DuPont Central Research and Development, Wilmington, DE 19880, USA

Abstract — We report on the effect of front-side Ag metallization on the underlying n^+p junction of multicrystalline Si solar cells. The junction quality beneath the contacts was investigated by characterizing the uniformities of the electrostatic potential and doping concentration across the junction, using scanning Kelvin probe force microscopy and scanning capacitance microscopy. We investigated cells with a commercial Ag paste (DuPont PV159) and fired at furnace setting temperatures of 800°, 840°, and 930°C, which results in actual cell temperatures ~100°C lower than the setting temperature and the three cells being under-, optimal-, and over-fired. We found that the uniformity of the junction beneath the Ag contact was significantly degraded by the over-firing, whereas the junction retained good uniformity with the optimal- and under-fire temperatures. Further, Ag crystallites with widely distributed sizes from <100 nm to several μm were found at the Ag/Si interface of the over-fired cell. Large crystallites were imaged as protrusions into Si deeper than the junction depth. However, the junction was not broken down; instead, it was reformed on the entire front of the crystallite/Si interface. We propose a mechanism of the junction-quality degradation, based on emitter Si melting at the temperature around the Ag-Si eutectic point during firing, and subsequent recrystallization with incorporation of impurities in the Ag paste and with formation of crystallographic defects during quenching.

Index Terms — Crystalline Si, solar cell, silver metallization, p - n junction, scanning Kelvin probe force microscopy, scanning capacitance microscopy.

I. INTRODUCTION

Front-side (FS) metallization is an important step in standard crystalline Si (c-Si) industrial cell production. Ag screen-printing is the most widely used contact-formation technique for commercial solar cells. The FS Ag contact grid is fabricated with screen-printing and rapid thermal processing (RTP). To date, two main current conduction models have been proposed [1]–[4]: electrical conduction through Ag crystallites formed at the grid/emitter interface and through Ag nano-colloid-assisted tunneling in the interfacial glass layer. The models are based on detailed structural observations using electron microscopy [1]–[4]; a clear understanding based on direct electrical measurements has not been achieved.

On the other hand, one concern is how Ag contact metallization affects the n^+p junction underlying the contact. This effect must be considered, along with its effect on the contact resistance ρ_c when optimizing the Ag paste and firing temperature. In this work, we investigate the electrical properties of the n^+p junction by imaging in two dimensions the electrostatic potential and local carrier density using the

atomic force microscopy (AFM)-based electrical techniques of scanning Kelvin probe force microscopy (SKPFM) [5] and scanning capacitance microscopy (SCM) [6]. We investigate the junction properties by examining the cells at under-, optimal-, and over-fired conditions.

II. EXPERIMENTAL

Detailed experimental conditions about the paste and cell making can be found elsewhere [7]. A standard commercial paste (DuPont, PV159) was screen-printed onto multicrystalline Si with a 65-ohm/square emitter. Over-firing conditions for a particular cell should depend on many factors such as the silver paste composition, furnace, firing profile, and belt speed. The three under-, optimal-, and over-fired cells investigated in this paper were fired at peak furnace setting temperatures of 800°, 840°, and 930°C, respectively, which are usually ~100°C higher than actual cell temperature.

For SKPFM and SCM cross-sectional sample preparations, a piece of the cell was glued with epoxy to a piece of Si wafer, with the front side of the cell facing the wafer. The cross-section was chemical-mechanically polished flat using a set of diamond pads and finally using silica colloids with fine particle sizes of ~50 nm. For the SCM measurement, an additional treatment of illuminating the sample with ultraviolet light while annealing at 300°C for 30 minutes helped to improve the quality of the oxide layer on the cross-sectional surface, which is critical for reliable SCM measurements [6].

SKPFM was based on non-contact-mode AFM in either ambient or an Ar glove box (Thermomicroscope CP and Veeco D5100&Nanoscope V), which give consistent results and thus excluded the effect of a water layer on the sample surface. The potential was measured by using the second harmonic frequency (300–400 kHz) of cantilever oscillation, which gives a potential resolution better than 20 mV. The AC voltage applied to the tip was 1 V. The back contact of the cell was grounded and the front contact was biased for changing voltage drop across the junction. Detailed SKPFM operation can be found in a previous publication [8].

SCM was based on contact-mode AFM in either ambient or an Ar glove box (Veeco D3100 or D5000 with Nanoscope V). An ultra high frequency (UHF) capacitance sensor was used for probing capacitance of the metal-insulator-semiconductor (MIS) structure consisting of the AFM tip, Si oxide layer, and

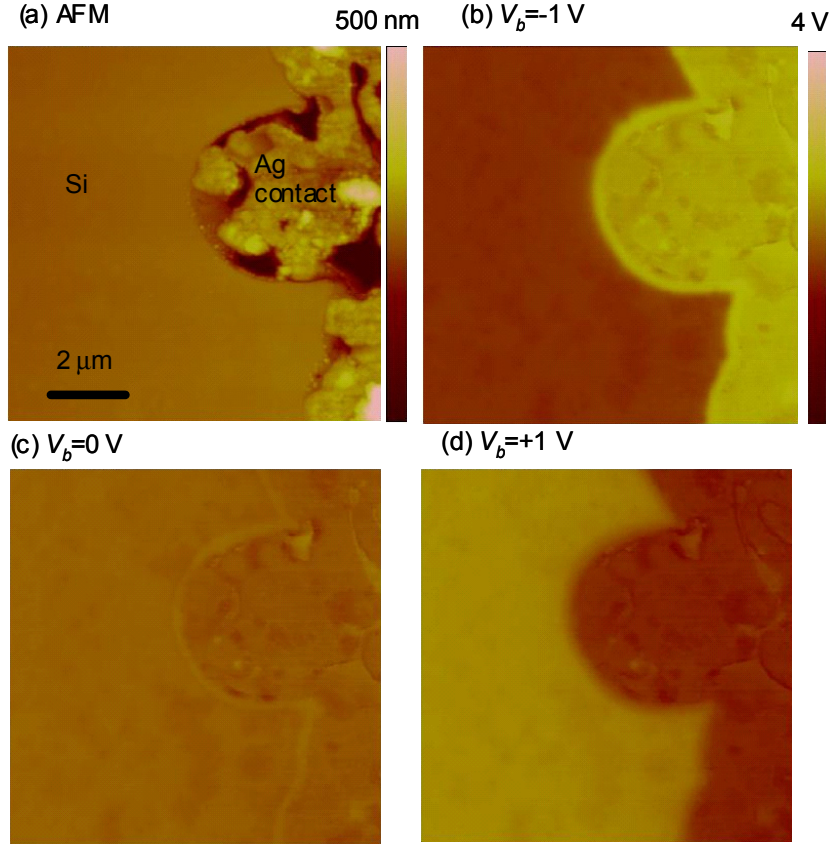


Fig. 1. (a) An AFM topographic and (b) (c) (d) the corresponding SKPFM potential images taken on the optimal-fired cell under $V_b = -1$, 0, and +1 V, respectively.

cross-sectional solar cell. The SCM signal (dC/dV) was measured using a lock-in amplifier and applying a 1-V AC modulating voltage to the sample. The front and back contacts of the cell were connected together. Detailed SCM operation can be found in a previous publication [9].

III. RESULTS AND DISCUSSIONS

We investigate the $n^+ - p$ junction quality beneath the contact grid by examining the two-dimensional potential distribution across the junction. Figure 1 shows an AFM topographic image and the corresponding SKPFM potential image taken on the optimal-fired cell under bias voltages of $V_b = -1$ V (reverse bias to the junction), 0 V, and +1 V (forward bias). Absolute potential values of Si bulk are all identical to the ground level, and the potential of Ag grid changes with V_b . The middle potential level shifts between the potential images to enhance the display of potential contrast. The AFM image can distinguish the boundary between the Si emitter and Ag grid, where sharp changes in the surface morphology occur [Fig. 1(a)]. One sees that the potential drop with changing V_b occurs mainly at a distance of ~ 400 nm from the Ag/Si interface, where the $n^+ - p$ junction of the diffused Si cell is

located. The potential changes are revealed more clearly by examining potential line profiles where the potential measurement was set at a constant line and V_b was swept (Fig. 2). With $V_b = 0$, the potential shows a small contrast (~ 0.1 V) across the junction [Fig. 2(a)]. This potential profile is primarily determined by the defect charges on the cross-sectional surface, rather than by the bulk property of the solar cell, because of Fermi level (E_F) pinning at the cross-sectional surface [8]. Although these defect charges determine the shape of the potential profile, the profile change with V_b depends mainly on the bulk property of the solar cell [8]. These potential changes are presented in Fig. 2(b) by subtracting the potential profile at $V_b = 0$ V from that at the various V_b values. One sees from Fig. 2(b) that the potential change with V_b is mainly on the $n^+ - p$ junction. The V_b -induced change in the electric field is further obtained by taking the derivative of the potential change [Fig. 2(c)]. The peak of the electric-field profile corresponds to the metallurgical junction [8]. In this specific location of the optimal-fired cell, the junction depth is ~ 380 nm. The junction depth determined in this way varies little, due to the angle of the cross-section with respect to the textured surface of solar cell and the accuracy of the methodology [8].

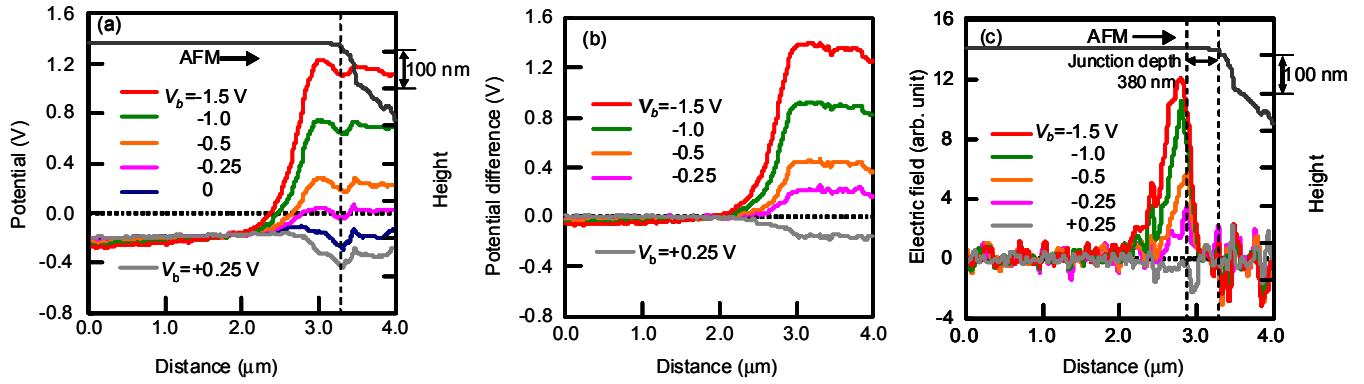


Fig. 2. (a) Potential profiles taken at a constant line position across the junction of the optimal-fired cell with various V_b values, (b) potential differences between the various V_b values and $V_b = 0$ V, and (c) profiles of the electric field induced by V_b . The corresponding AFM line profile is also shown.

The potential distribution across the junction and the junction depth of the optimal-fired cell are uniform parallel to the textured Si emitter surface, as shown in Fig. 1. The distribution of the depletion width is also uniform. The junction is conformal with the surface morphology of the cell. Therefore, the junction in this cell retains good quality, not noticeably damaged by the screen-printing of Ag paste and firing. The junction depletion width is ~ 650 nm as estimated from the electric-field extension [Fig. 2(c)]. It is

semiquantitatively consistent with the depletion width in the bulk when applying $V_b = -1.5$ V to the device [8]. The remaining difference is mainly due to the long-range nature of the Coulomb force between the tip and sample [8,10].

Potential distribution of the over-fired cell shows high nonuniformity, i.e., the junction depth and depletion width change with the junction location [Figs. 3(a) and 3(d)]. From the AFM images, Ag crystallite-like features can be identified, consistent with the electron microscopy observations [1]–[3].

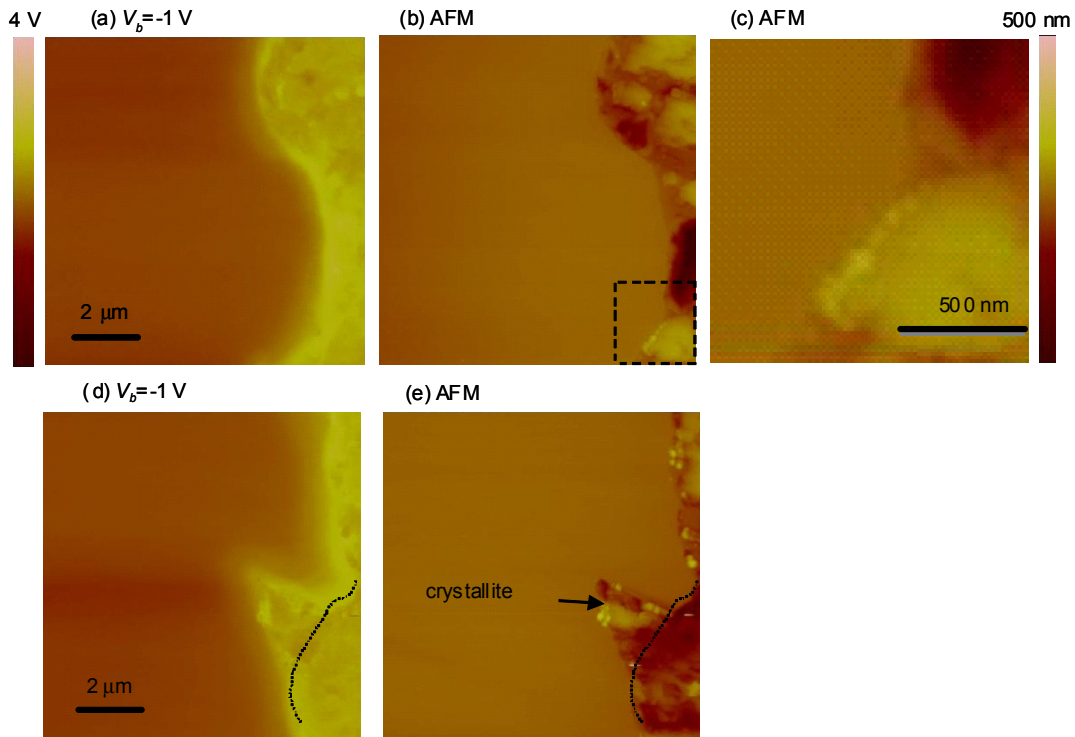


Fig. 3. (a) SKPFM potential and (b) (e) the corresponding AFM images taken on the over-fired cell in areas (a) (b) without and (d) (e) with large crystallites. (c) is a close-up of the dashed square in (b).

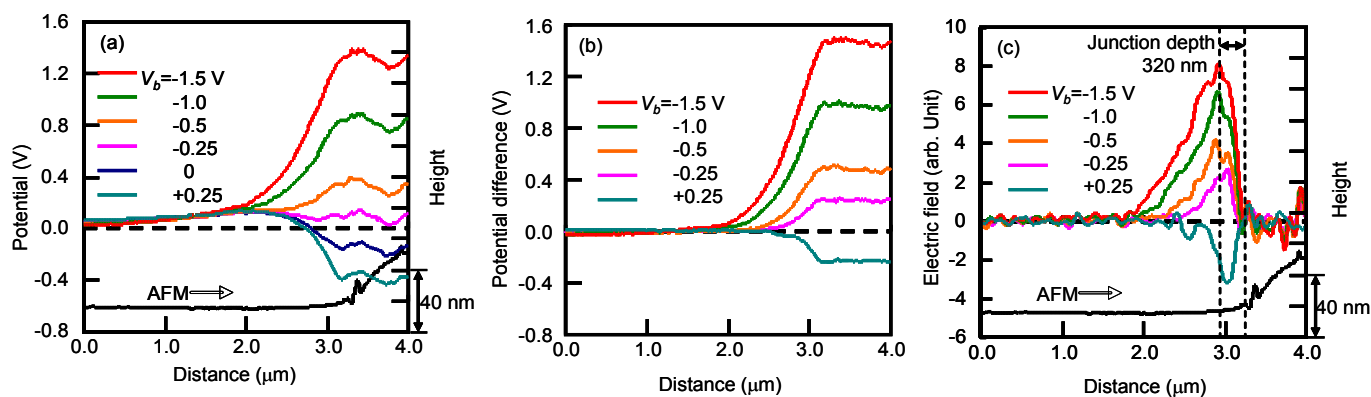


Fig. 4. (a) Potential profiles taken at a constant line position across the junction of the over-fired cell with various V_b values, (b) potential differences between the various V_b values and $V_b = 0$ V, and (c) profiles of the electric field induced by V_b . The corresponding AFM line profile is also shown.

The size of the Ag crystallites ranges widely from <100 nm to a few μm . Examples of small and large crystallites are shown in Figs. 3(c) and 3(e), respectively; Figure 3(c) is a close-up of the dashed square area in Fig. 3(b). In most cases, the small crystallites appear to attach to or slightly embed in the emitter at the Si/grid interface [Fig. 3(c)]; in contrast, large crystallites protrude or deeply embed into the emitter [Fig. 3(e)].

The overall nonuniform potential distribution [Figs. 3(a) and 3(d)] beneath the Ag contact indicates a commonly damaged junction by the over-firing. The junction quality degrades significantly compared with the optimal-fired cell. However, it is surprising that although the large crystallites are deeply embedded into the emitter—e.g., on the order of μm deep, which is much deeper than the junction depth (~ 380 nm)—the crystallites do not break down the junction; instead, the junction is driven into the bulk, as revealed by the potential image [Fig. 3(d)]. If the junction were broken down, a shunt would be created. The potential image would be much different. The fact that the potential drops beneath the large crystallites at a similar distance from the Ag/Si interface to the region without the large crystallite indicates that the junction is driven into the bulk (as also seen later by SCM measurement).

Example potential profiles taken at a constant line position of the over-fired cell are shown in Fig. 4(a), which were taken at a location without the large Ag crystallite. The electric field profiles [Fig. 4(c)] exhibit significantly wider depletion width (~ 1 μm) and shallower junction depth (~ 320 nm) than the optimal-fired cell. The potential and electric field profiles vary with the junction location, consistent with the degraded potential uniformity (Fig. 3). Broadening of depletion width was commonly observed in this over-fired cell. However, the change in junction depth is not well defined, and is not as

significant as the depletion width. These junction characteristics of the over-fired cell indicate a broadening of the n -doping profile and a reduction in the overall doping density beneath the Ag grid.

The junction degradation is caused by interactions of Ag paste with the Si emitter at the raised temperature, but not by thermal effects during firing. The potential taken in regions away from the Ag grid is distributed uniformly (the images are not shown), which agrees with the discussion above. The dopant concentration is not expected to redistribute with an $\sim 830^\circ\text{C}$ actual cell peak temperature (930°C furnace setting temperature) and a short dwelling time of less than 30 seconds, considering the normal emitter diffusion temperature of $900^\circ\text{--}1100^\circ\text{C}$ and diffusion time of ~ 10 minutes, for the diffused cell [11].

Incorporation of impurities into the junction during over-firing is considered to be a main reason for the junction degradation. The actual over-fired cell temperature of $\sim 830^\circ\text{C}$ is at about the Si-Ag eutectic temperature ($\sim 835^\circ\text{C}$) [12]. A considerable amount of Ag was probed in Si beneath the Ag grid [12], and the amount should be sensitive to the firing temperature around the eutectic temperature. A possible mechanism is that in over-firing conditions around the eutectic temperature, the Ag paste chemistry etches away the SiNx:H layer and further forms a Ag-Si liquid with Si. As the cell passes the firing furnace after peak firing temperature, the cell temperature drops sharply. During this quenching, Si and Ag phases segregate and crystallize from the Ag-Si liquid. The widely distributed Ag crystallite sizes may result from variations of local Ag concentration in the Ag-Si liquid and/or local fluctuation of Si melting depth when the cell is at high temperature around the Ag-Si eutectic point.

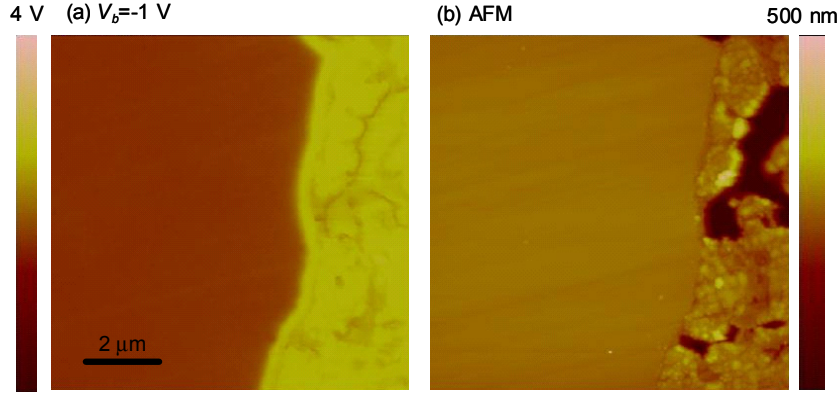


Fig. 5. (a) a SKPFM potential and (b) the corresponding AFM images taken on the under-fired cell under $V_b = -1$ V.

Recrystallized Si from the melt contains the emitter dopants, and the junction is reformed. The recrystallized Si could contain a large amount of Ag and other impurities. Ag impurity in Si creates pseudo-donor levels that could increase dark saturation current and the diode ideality factor [13]. Other metal impurities are also detrimental to the junction quality. In addition, significant crystallographic defects could be created during the Si recrystallization, which is another reason for junction degradation. Significant η_{eff} degradation was measured with this over-fired cell, mainly manifested as degradation of fill factor (FF) [1,7]. Increase in series resistance (R_s) is responsible for part of this FF degradation [1,7]. Both contact resistance ρ_c and the emitter sheet resistance (R_{sh}) beneath the grid could be degraded by the over-firing. Another part of FF degradation can be attributed to the degradation of junction-quality/leakage-current or pseudo-FF [14]. Our observation of the degraded junction uniformity is consistent with the degradations in both pseudo-FF and R_{sh} under the grid.

The potential distribution of the under-fired cell is undisturbed (Fig. 5), as expected. The potential distributions on the emitter, junction, and absorber, as well as the junction depth and depletion width, are all uniform.

We further measured the carrier distribution on the optimal- and over-fired cells using SCM (Fig. 6) and obtained results consistent with the potential measurements. Because the Ag grid is in contact with a highly n-doped emitter surface ($\sim 10^{21}/\text{cm}^3$), the grid/emitter interface is not discernible from the SCM image due to the near-zero signal strength on both regions. The grid/emitter boundary curves in Fig. 6 are drawn according to the AFM images and superimposed onto the SCM image. Figures 6(a) and 6(b) were taken on the optimal-fired cell. The emitter doping and the junction depth are uniform, which indicates a high-quality junction, consistent with the SKPFM measurements.

The doping uniformity degrades significantly on the over-fired cell, as revealed in Figs. 6(c) and 6(d) taken on a region without large Ag crystallites. This image also shows a widening of the dark region, corresponding to widening of the lightly n-doped and depletion regions, consistent with the potential image of Fig. 3(a). Figures 6(e) and 6(f) were taken on a region with a large Ag crystallite. The curves are drawn by assuming the grid/emitter boundary before metallization. The image shows that the large crystallite does not break down the junction, and the emitter doping exists in the entire front of the crystallites, again consistent with the potential measurements shown in Fig. 3(d). The image shows clear uniformity degradation compared with the optimal-fired cell [Fig. 6(a)].

IV. SUMMARY

Three multicrystalline Si solar cells, with a commercial Ag paste and being over-, optimal-, and under-fired at furnace setting temperatures of 930°, 840°, and 800°C, were subjected to the investigation of the effect of FS Ag screen-printing metallization on the underneath n^+p junction. The actual cell peak temperature was $\sim 100^\circ\text{C}$ lower than the setting temperature. The over-firing significantly degraded the underlying junction quality, as manifested by the nonuniformly distributed potential and carrier concentration across the junction. The optimal- and under-firing retained the good junction quality similar to the areas away from the Ag grid. With this over-fired cell, a large amount of Ag crystallites with sizes from <100 nm to a few μm were found at the Ag/Si interface. Large Ag crystallites were imaged as protruding deeply into the Si emitter, deeper than the junction depth. However, the junction was not broken down by the crystallites; instead, a degraded junction was reformed. We proposed a mechanism of the junction degradation, based on Si recrystallization from Ag-Si melting mixture with

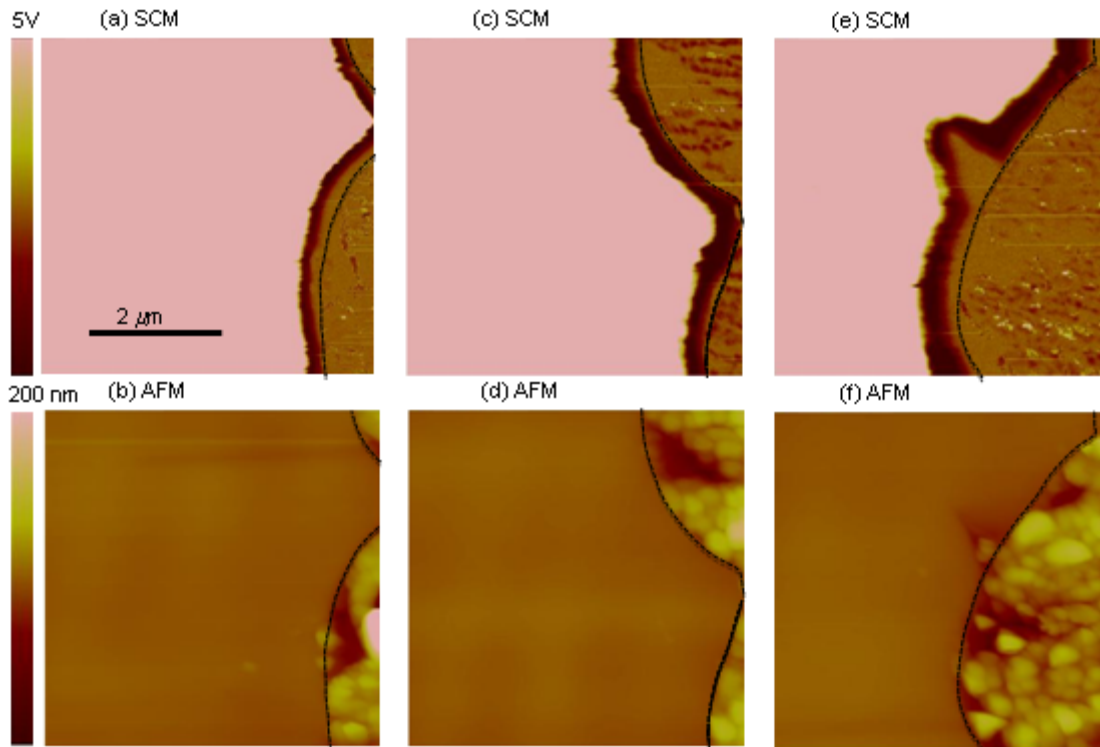


Fig. 6. (a) (c) (e) SCM and (b) (d) (f) the corresponding AFM images taken on (a) (b) the optimal-fired cell, and on the over-fired cell in regions (c) (d) without and (e) (f) with the large crystallite.

incorporation of impurities in the Ag paste and with formation of crystallographic defects. The effects of this junction degradation on solar cell performance were discussed.

ACKNOWLEDGEMENTS

NREL authors thank the U.S. Department of Energy for funding under Contract No. DE-AC36-08GO28308. We are grateful to DuPont colleagues L.K. Cheng, K.E. Mikeska, C.C. Torardi, D.H. Roach, P.D. VerNooy, F. Gao, R. Getty, A. Carroll, B. Laughlin, W. Borland, P. O’Callaghan, R.A. Leach, K.E. Myers, and J.A. Sternberg for fruitful discussion throughout this investigation, and to B. Fish for technical assistance.

REFERENCES

[1] Z.G. Li, L. Liang, A.S. Ionkin, B.M. Fish, M.E. Lewittes, L.K. Cheng, and K.R. Mikeska, *J. Appl. Phys.* 110, 074304 (2011).
 [2] Z.G. Li, L. Liang, and L.K. Cheng, *J. Appl. Phys.* 105, 66102 (2009).
 [3] C. Ballif, D. Huljic, G. Willeke, and A. Hessler-Wyser, *Appl. Phys. Lett.* 82, 1878 (2003).

[4] M.M. Hilali, K. Nakayashiki, C. Khadikar, R.C. Reedy, A. Rohatgi, A. Shaikh, S. Kim, and S. Sridharan, *J. Electrochem. Soc.* 153, A5 (2006).
 [5] M. Nonnenmacher, M.P. O’Boyle, and H.K. Wickramasinghe, *Appl. Phys. Lett.* 58, 2921 (1991).
 [6] For a review, see C.C. Williams, *Annu. Rev. Mater. Sci.* 29, 471 (1999).
 [7] A.S. Ionkin, B.M. Fish, Z.G. Li, M.E. Lewittes, P. Soper, J.G. Pepin, and A.F. Carroll, *ACS Applied Materials & Interfaces* 3, 606 (2011).
 [8] C.-S. Jiang, H.R. Moutinho, R. Reedy, M.M. Al-Jassim, and A. Blosse, *J. Appl. Phys.* 104, 104501 (2008).
 [9] C.-S. Jiang, J.T. Heath, H.R. Moutinho, and M.M. Al-Jassim, *J. Appl. Phys.* 110, 014514 (2011).
 [10] Y. Shen, D.M. Barnett, and P.M. Pinsky, *Rev. Sci. Instrum.* 79, 023711 (2008).
 [11] F. Lasnier and T.G. Ang, *Photovoltaic Engineering Handbook* (Adam Hilger, New York, NY, USA, 1990), pp. 43–46.
 [12] D.L. Meier, H.P. Davis, R.A. Garcia, J.A. Jessup, and A.F. Carroll, *Proc. of 28th IEEE PVSC (Anchorage, Alaska, USA, Sept. 15–22, 2000, IEEE, Piscataway)*, p. 69.
 [13] N.T. Son, M. Singh, J. Dalfors, B. Monemar, and E. Janzen, *Phys. Rev. B* 49, 17428 (1994).
 [14] R.A. Sinton and A. Cuevas, *Proc. of the 16th European Solar Energy Conference (Glasgow, UK, May 1–5, 2000)*, p. 115.